Photoswitchable Merocyanine-Amphiphiles with Programmable Self-Assembly Times

ChemEurJ

Research Article
doi.org/10.1002/chem.202502399

Chemistry Europe
European Chemical Societies Publishing

www.chemeurj.org

Photoswitchable Merocyanine-Amphiphiles with Programmable Self-Assembly Times

Man Him Chak,[a] Laura Wimberger,[a] Bailey Richardson,[b] Natalie E. Newman,[a] Emma M. V. Johansson,[c] Jake P. Violi,[a] Anna Sokolova,[d] Hendrick Frisch,[b] Felix J. Rizzuto,[a] William A. Donald,[a] Martina H. Stenzel,[a] Joakim Andréasson,[e] and Jonathon E. Beves*[a]

A merocyanine-based amphiphile was self-assembled into ellipsoids that can be disassembled by irradiation with visible light and reassemble in the dark after a delay of ~70 minutes. Above a threshold concentration, the reassembly occurs when the ratio of protonated merocyanine to spiropyran reaches 7:3, suggesting both isomers are involved in the assembly. The thermal isomerization of the amphiphile when assembled (half-life ~13 minutes) is significantly slower than that in dilute solution (half-life ~3.6 minutes). The self-assembly behavior was confirmed by UV-vis spectroscopy, dynamic light scattering (DLS), small-angle neutron scattering (SANS) and small-angle X-ray scattering (SAXS). The delay between the isomerization and the assembly processes can be tuned between minutes and hours by adding differently charged co-surfactants.

1. Introduction

Amphiphiles can self-assemble into structures with diverse functions, including for drug delivery,[1] to act as actuators,[2] or hydrogels.[3] Where the amphiphiles are suitably responsive molecules, these self-assemblies can be dynamically controlled, for example, by pH,[4] temperature,[5] redox reactions,[6] or light.[7] Light is a convenient means for manipulating chemical systems, as it provides high spatial and temporal precision and allows for noninvasive remote control.[8] One way to introduce photo-responsiveness is by using molecular photoswitches. A variety of photoswitches have been incorporated into amphiphile self-assembled systems, including azobenzenes,[9] arylazopyrazoles,[10] indigos,[11] dithienylethenes,[12] and spiropyran/merocyanines.[13] Spiropyrans[13c,f] have the advantage that their polarity and the overall charge change upon isomerization between the spiropyran and the merocyanine forms, resulting in significant changes to self-assembly properties. Spiropyran amphiphiles can assemble at interfaces,[13l,m] or form liquid crystals,[13n] micelles,[13d] or vesicles.[13e] Such photoresponsive materials can have functions including for cargo delivery[13m] or foam stabilization.[13h] The photo- and thermal-switching properties of photoswitches can change significantly when they are no longer in free solution.[14] For example, thermal isomerization rates can be strongly altered when the photoswitch is bound within a cavity,[15] or by binding a guest[16] or transition metal ion,[17] or by being aggregated.[18] A seminal matter to understand in studying photocontrolled self-assembly of any type is how the photoinduced and the thermal isomerization rates of the photoswitch correlate with the corresponding assembly/disassembly rates of the structures. In some cases, the rates monitored by UV-vis spectroscopy (reflecting isomerization rates) match the corresponding rates measured by techniques such as small-angle X-ray scattering (SAXS)/small-angle neutron scattering (SANS)[19] (reflecting assembly/disassembly rates), strongly suggesting that the formation of the structures is directly controlled by the isomerization of the photoswitch. In other examples, isomerization and assembly/disassembly occur at different rates,[20] allowing for the formation of transient structures and interesting nonlinear behavior.

Herein we report a photoswitchable merocyanine which self-assembles into ~100 nm structures in the dark and disassembles upon visible light irradiation (Figure 1). Unlike previous photoswitchable assemblies, there is a long delay (~70 minutes) between when the light is switched off and when the self-assembly occurs. Once above a threshold concentration,

[a] M. H. Chak, Dr. L. Wimberger, N. E. Newman, Dr. J. P. Violi, Dr. F. J. Rizzuto, Prof. W. A. Donald, Prof. M. H. Stenzel, Prof. J. E. Beves
School of Chemistry, UNSW Sydney, Sydney NSW 2052, Australia
E-mail: j.beves@unsw.edu.au

[b] B. Richardson, Prof. H. Frisch
School of Chemistry and Physics, Queensland University of Technology, 2 George Street, Brisbane QLD 4000, Australia

[c] Dr. E. M. V. Johansson
Flow Cytometry Facility, Mark Wainwright Analytical Centre, UNSW Sydney, Sydney NSW 2052, Australia

[d] Dr. A. Sokolova
Australian Centre for Neutron Scattering, Australian Nuclear Science and Technology Organisation (ANSTO), New Illawarra Road, Lucas Heights NSW 2234, Australia

[e] Prof. J. Andréasson
Department of Chemistry and Chemical Engineering, Chalmers University of Technology, Göteborg 412 96, Sweden

Supporting information for this article is available on the WWW under https://doi.org/10.1002/chem.202502399

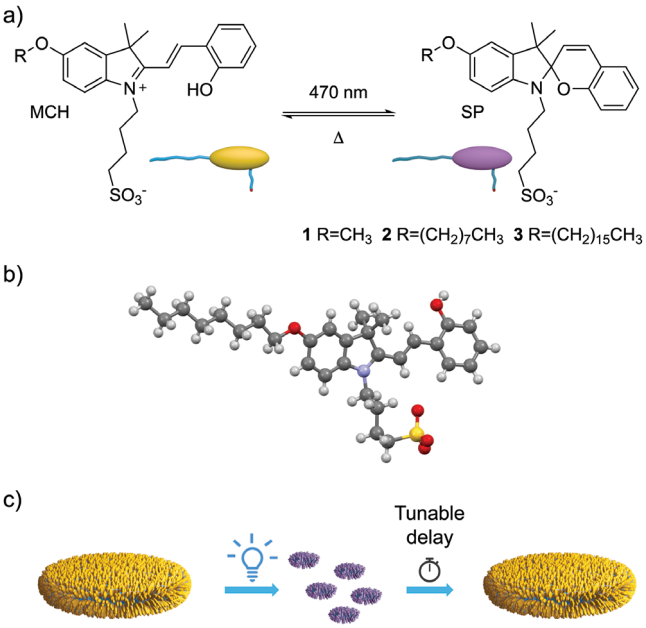

Figure 1. a) Photoswitchable merocyanines **1–3**. b) Single X-ray crystal structure of **2**-MCH. c) Photoswitching of the self-assembly of compound **2**.

the delay is largely independent of the concentration and is tunable from 40 minutes to 3 hours via the addition of a co-surfactant.

2. Results and Discussion

We designed two new merocyanine amphiphiles based on a merocyanine photoacid **1**, which is able to generate basic-to-acid pH changes.[21] The merocyanine scaffold was chosen as it can be operated with visible light, displays good water solubility and fatigue resistance. To form an amphiphile for self-assembly, the methoxy group on the indole moiety of **1** was replaced with 8- or 16-carbon hydrocarbon chains, giving compounds **2** and **3**, respectively (see Supporting Information-1 to Supporting Information-2 for details). Compound **3** has poor solubility in water, or even pure DMSO, and cannot act as a useful amphiphile, so was excluded from further experiments.

A single-crystal X-ray structure of **2** confirmed the expected *trans*-configuration and a molecular length of 2.4 nm (Supporting Information-2.6.1). Packing of compound **2-MCH** in the solid state displayed a strong intermolecular hydrogen bond between the phenol OH and the sulfonate group (O···O distance of 2.600(2) Å), which could also be important when self-assembled in the aqueous phase. Surprisingly, the molecules do not pack with close contacts between the greasy chains, with other intermolecular interactions dominating the packing (Supporting Information-2.6.1, Figure S14).

The optical and photoswitching properties of compound **2** were characterized in aqueous solutions (20 μM with 0.5% v/v DMSO, Supporting Information-3, Supporting Information-4, Supporting Information-5) using reported methods.[22] The effective pK_a values of compound **2** in the dark (pK_a^{dark} = 7.5, Supporting Information-4.1) and under irradiation with 467 nm light ($pK_a^{h\nu}$ = 3.2, Supporting Information-4.1) are similar to those of the parent merocyanine **1**.[21] At pH 4.8 and low concentration (9 μM), compound **2** is almost quantitatively in its protonated merocyanine form (**2-MCH**) in the dark, as measured by UV-vis spectroscopy (Supporting Information-4.3, Table S3). When irradiated with 467 nm light, it is almost exclusively (94%) in the spiropyran form **2-SP** (Supporting Information-5.2, Table S4).[21] This is consistent with the expected photophysical properties being similar between the methoxy and any alkoxy derivative. At pH 4.8, where the **2-MCH** form dominates, the visible absorption maximum is at 437 nm, consistent with that for **1-MCH** (434 nm[21]). A sample of **2** at high pH (pH 11.8) shows the visible absorption of the MC form is centered at 533 nm (Supporting Information-4.1, Figure S24), again consistent with that for compound **1-MC** (528 nm[21]). The thermal isomerization rate is strongly pH dependent, as expected,[22,23] and the thermal half-life of compound **2-SP** was determined to be ~3.6 minutes at pH 4.8 and 9 μM (Supporting Information-5.4, Table S6). This is consistent with the reported value for compound **1-SP** (4.1 minutes, pH 4.61).[21] At higher concentrations, we expect these amphiphiles to self-assemble and their switching properties to change.

2.1. Self-assembly Behavior of Amphiphile 2

To study the self-assembly behavior of **2-MCH,** we used dynamic light scattering (DLS) to determine the critical aggregation concentration (CAC) (0.5% DMSO/water (v/v),[24] buffered at pH 4.8; see Supporting Information-6.1). The derived count rates were measured in the dark for **2**, ranging from 7 μM to 284 μM (Figure 2a). From this data, we estimate a CAC for compound **2** at pH 4.8 to be 25 μM. When the concentration of **2** increased beyond 200 μM, the derived count rate plateaus, suggesting more complicated aggregation behavior at higher concentrations. In the dark, DLS data indicated that compound **2** forms

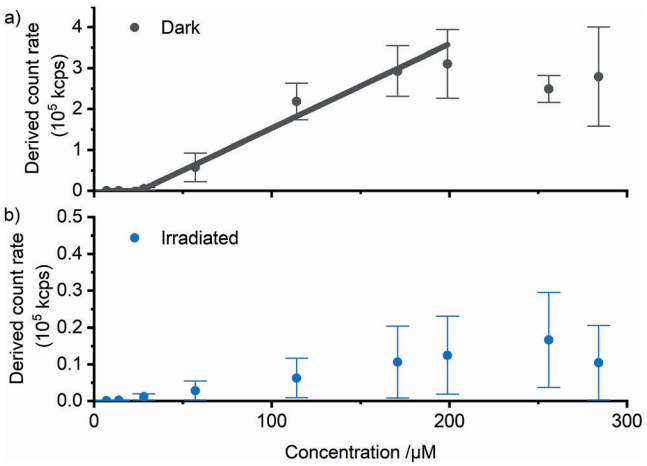

Figure 2. Change in the derived count rate of increasing concentrations of compound **2** a) in the dark and b) immediately after irradiation, monitored by DLS. Experimental conditions: 0.5% DMSO in water; [phosphate buffer] = 20 mM; pH 4.8, irradiation time = 15 min, λ = 467 nm, *T* = 25 °C.

self-assemblies with a diameter around ~100 nm (Figure 3d). Cryo-transmission electron microscopy (CryoTEM) and transmission electron microscopy (TEM) images of the assemblies are consistent with large assemblies in the dark (Supporting Information-9 Figure S54, S55). All subsequent studies were conducted with a concentration of **2** of 190 μM, where stable assemblies appeared to be formed. At such high concentration, a new red-shifted absorption shoulder is observed, centered around 520 nm, close to where **2-MC** absorbs (533 nm, Supporting Information-5.1, Figure S26). This suggests that when **2** is aggregated, the pK_a of **2-MCH** is lower, favoring the formation of **2-MC**, which in turn implies formation of **2-SP** in thermal equilibrium with **2-MC**.

Both **2-SP** and **2-MC** have stronger absorption at 250 nm than **2-MCH**, so some caution is required when using the UV absorption to estimate speciation. The stabilization of the SP isomer has been previously shown for spiropyran compounds interacting with membranes,[25] and concentration-dependent equilibria between MCH and SP have been reported.[13i,26] Absorption at longer wavelengths (>600 nm) is consistent with scattering from particles, which we will also use as a proxy for particle formation.[27]

2.2. Photoswitching of Self-assembled Amphiphile 2

The self-assembly of amphiphile **2** in the dark and under irradiation was characterized by UV-vis spectroscopy, DLS, SANS, SAXS, and CryoTEM. When a sample of **2** (190 μM, pH 4.8) was irradiated with 467 nm light for 15 minutes, the absorbance at 437 nm, characteristic of **2-MCH**, decreases while the absorbance at 250 nm, characteristic of **2-SP** (and **2-MC**), increases (Figure 3a), as expected for MCH→SP isomerization.[28] The decrease in absorbance at 437 nm corresponds to 84% of **2-MCH** being isomerized to **2-SP** upon irradiation (Supporting Information-5.2, Table S4), which is less than that found for dilute (9 μM) samples of **2** (94%, pH 4.8, Supporting Information-5.2, Table S4). This effect is likely caused by the formation of **2-MC** in the aggregates. Compound **2** (9 μM) showed poor photoswitching at pH 11.8, where **2-MC** is the dominant form (52% switched, Supporting Information-5.2, Figure S29, Table S5). The quantum yield of photoinduced ring closing of related MC compounds is low compared to that of MCH, suggesting most photoswitching is due to absorption by trace MCH.[22b] Prolonged irradiation did not result in further photoswitching from **2-MCH** to **2-SP** but decomposition of compound **2**, presumably by established hydrolysis pathways from the **MC** form[28] (Supporting Information 5.6, Figures S35 and S36).

After irradiation with 467 nm light, the measured DLS data had a significant decrease in the derived count rate and is consistent with the formation of some smaller assemblies with diameters of 20–50 nm (Figure 3b,d). The derived count rate is much lower than that in the dark, and there is no clear CAC observed for concentrations between 7 μM and 280 μM (Figure 2).

SANS was measured on a sample of **2** in the dark (190 μM, pH 4.8). The resulting scattering profile was fit as oblate ellipsoids, similar to reported anisotropic assemblies.[29] The polar and equatorial radii were estimated to be 17.0 ± 0.5 nm and 91.0 ± 1 nm, respectively (Supporting Information-7, Table S9). Upon irradiation with 445 nm light, a significant decrease in the scattering intensity was observed between the Q range of 0.003-0.03 Å^{-1}, along with a change in scattering profile (Supporting Information-7, Table S9). The decrease in scattering intensity is consistent with the formation of smaller objects, and the scattering profile could not be reasonably fit to the ellipsoid model.

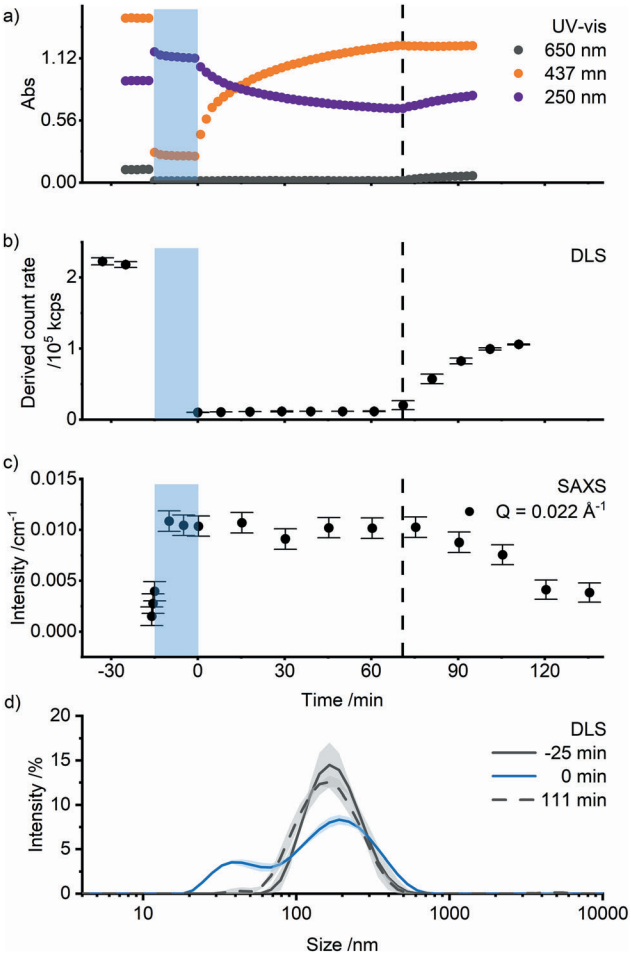

Figure 3. Photoswitching of compound **2** self-assembly. a) Change in characteristic absorbance measured by UV-vis spectroscopy of **2-MCH** (orange) and **2-SP** (purple) upon and after irradiation ([**2**] = 190 μM, 467 nm, 5 min). b) Derived count rate monitored by DLS of compound **2** self-assembly solution ([**2**] = 190 μM) before and after irradiation. c) SAXS scattering intensity of solution of compound **2** ([**2**] = 570 μM) Q = 0.02215 Å−1 before and after irradiation. d) Size distribution of compound **2** self-assembly ([**2**] = 190 μM) measured by DLS before and after irradiation. Experimental conditions: 0.5% DMSO/water, pH = 4.8, [phosphate buffer] = 20 mM, T = 25 °C, irradiation time = 15 min, λ = 467 nm. Irradiation time is indicated with a light blue rectangle. The vertical dashed line indicates 71 minutes after the light is switched off.

2.3. Thermal Re-assembly of Amphiphile 2

We monitored the thermal recovery of these assemblies in the dark by UV-vis absorption to verify that the light-induced

assembly changes of amphiphile **2** are reversible (Figure 3a). A sample of compound **2** (190 μM in 0.5% DMSO/water (v/v) buffered at pH 4.8) was irradiated at 467 nm for 15 minutes. After the light was switched off, the absorbance at 437 nm gradually increases, while the absorbance at 250 nm decreases, consistent with the thermal recovery of **2-SP** → **2-MCH** (Figure 3a). The apparent half-life of compound **2-SP** at 190 μM is ~13 minutes (Supporting Information-5.4, Table S6) and is approximately constant from 47 to 379 μM (Figure 4, Supporting Information-5.4, Table S6) and significantly longer than that of more diluted samples (9 μM, ~3.6 minutes, Supporting Information-5.4, Table S6). This indicates that the self-assembly process influences the rate of the thermal isomerization of **2-SP**→**2-MCH**.

More interestingly, after ~70 minutes in the dark, the absorbance at 250 nm rapidly increases, together with apparent absorbance at 650 nm, which is consistent with scattering by particles.[27] We attribute this change to the self-assembly of the large structures, which change the local environment of the photoswitch. This is supported by the simultaneous increase in the derived count rate measured by DLS as the smaller assemblies disappear (Figure 3b, Supporting Information-6.2, Figure S39) and the structure profile changes in SAXS after irradiation (Figure 3c, Supporting Information-8, Figures S51 and S53). This demonstrates that the photoinduced morphological change of the self-assemblies of amphiphile **2** is reversible. The increase in absorbance at 250 nm after 70 minutes in the dark (Figure 3a) is consistent with isomerization from **2-MCH** → **2-SP**, but deprotonation of **2-MCH** to form **2-MC** may also be a reasonable explanation.[30]

A delayed (dis)assembly response (~2 minutes) has been reported for a lipid-azobenzene surfactant mixed system,[20a] suggesting the behavior we have observed could be general to other switchable amphiphiles. To the best of our knowledge, this is the first example of self-assembly of merocyanine-based amphiphile with a long (>1 hour) delay between thermal isomerization and assembly rearrangement. The ability to program a structural change in the materials ahead of time could be useful in creating complex molecular systems with nonlinear kinetics.

After 6 hours in the dark, the SANS scattering profile recovered and was fit to the ellipsoid model with dimensions (polar radius: 11.3 ± 0.2 nm, equatorial radius: 77.0 ± 1.0 nm, Supporting Information-7, Table S9) comparable to the assemblies before irradiation. SAXS data (Supporting Information-8, Figure S51) also showed a change in the scattering profile after irradiation, which recovered in the dark after ~70 minutes (Figure 3c). These results suggest that upon irradiation, self-assemblies of amphiphile **2-MCH** rearrange from oblate particles with sizes of ~100 nm to smaller aggregates with diameters of 20–50 nm, and the larger aggregates reform in the dark after ~70 minutes.

From the measured pK_a values in dilute solutions, we expect compound **2** to be almost pure **2-MCH** in the dark at pH 4.8 (Supporting Information-4.3, Table S3). However, the formation of self-assembled structures could create hydrophobic environments that favor the conversion of **2-MCH** to the more apolar **2-SP**. The polarity change of the environment was detected using Prodan dye, for which the wavelength of maximum emission is strongly polarity dependent. When self-assembled with compound **2**, the emission maximum of Prodan is 538 nm. After irradiation with 467 nm light, the emission maximum shifted to 527 nm,[31] consistent with Prodan dye being in a less polar environment (Supporting Information-10, Figure S58). The surface charge of the particles could provide information about their composition because **2-SP** and **2-MC** are anionic, while **2-MCH** is zwitterionic. Using electrophoretic light scattering (ELS), we measured the zeta potential of the self-assemblies (Supporting Information-6.5, Figure S46). A 190 μM sample of **2** in the dark gave a measured zeta potential of −76 mV, which decreased to −82 mV upon irradiation with 467 nm light and gradually recovered to its original value after the light was removed (Supporting Information-6.5, Figure S46). The presence of anionic **2-SP/2-MC** in the ellipsoids in the dark is consistent with the negative zeta potential observed in these assemblies.

2.4. Concentration Dependence of Ellipsoid Reformation

The concentration-dependence of the self-assembly process was investigated by UV-vis absorption spectroscopy. We prepared samples of compound **2** with concentrations between 2.25 μM and 379 μM and monitored their thermal recovery after irradiation by 467 nm light for 15 minutes (Figure 4). For samples of **2** below the CAC (<25 μM), there is no rapid increase in the absorbance at 250 nm during the thermal recovery. This is consistent with no large self-assemblies being formed. For samples of **2** with concentrations higher than the CAC, ~70 minutes after the light is switched off there is a rapid increase in absorbance at 250 nm and, consistent with scattering by large particles, at 650 nm. To our surprise, there is no significant difference in the time required for this increase in absorption to occur with concentrations of **2** ranging from 47 μM to 379 μM. This unexpected result indicates that the assembly process depends on the concentrations of both **2-SP** and **2-MCH**, and not only the

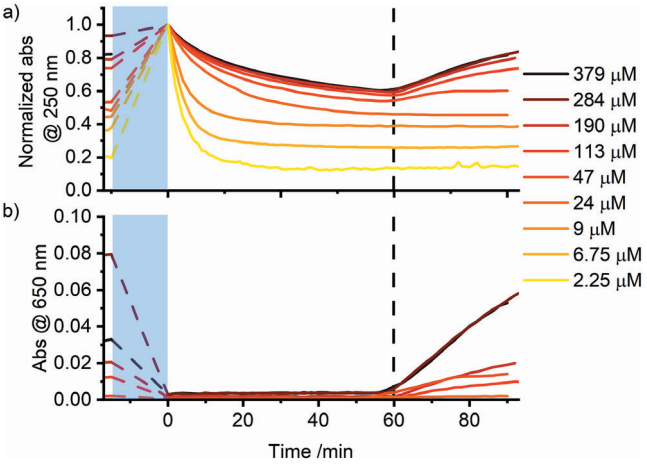

Figure 4. Recovery of absorbance at a) 250 nm, characteristic of **2-SP**, normalized to absorbance immediately after irradiation (raw data presented in Supporting Information-5.4, Figure S31) and b) 650 nm after irradiation. Concentrations of **2** in 0.5% DMSO/water, pH = 4.8, [phosphate buffer] = 20 mM, T = 25 °C, irradiation time = 15 min, λ = 467 nm. Irradiation time is indicated with a light blue rectangle.

concentration of **2-MCH**, consistent with the assembly requiring a certain ratio of **2-MCH** and **2-SP**. We estimated that ~30% **2-SP/MC** is required for the reassembly of the oblate ellipsoids, based on the absorbance at 437 nm (Supporting Information-5.4, Table S6). The zwitterionic **2-MCH** that exists in the dark might be expected to pack into bilayer structures, such as those found in a liposome or a disc.[32] Under irradiation the anionic species formed (**2-SP**/**2-MC**) would be repulsive to each other and would be expected to form smaller aggregates with a higher surface curvature to allow the negative charges to be further apart and screened by solvent. The involvement of **2-SP**/**2-MC** in the self-assembly is corroborated by the negative zeta potential on assemblies formed in the dark from zwitterionic **2-MCH** (Supporting Information-6.5, Figure S46).

2.5. Programming Delay with Co-Surfactants

To investigate the effect of charge on the self-assembly of compound **2**, we added co-surfactants that were cationic (cetyltrimethylammonium bromide = CTAB) or anionic (sodium dodecyl sulphate = SDS). Spiropyran derivatives have been previously assembled with cosurfactants, such as cetyltrimethylammonium chloride, to act as molecular logic gates,[20c] or polyethylene glycol derivatives for drug delivery.[13b]

We doped self-assemblies of compound **2** with 19 μM (0.1 eq. w.r.t. **2**) or 48 μM (0.25 eq. w.r.t. **2**) of either CTAB or SDS under the same conditions described in previous sections. The samples were irradiated with 467 nm light for 15 minutes, and the thermal recovery was monitored by UV-vis (Figure 5, Supporting Information-5.5, Figures S33 and S34) and DLS (Supporting Information-6.5, Figure S45, S46). The concentration of CTAB and SDS used in these experiments is well below their respective CACs (Supporting Information-6.3 and Supporting Information-6.4).[33] The addition of 0.1 eq. or 0.25 eq. of CTAB shortens the delay to about 40 minutes or 25 minutes, respectively. The addition of 0.1 eq. or 0.25 eq. of SDS lengthens the delay to 100 minutes or 205 minutes, respectively (Figure 5, Supporting Information-5.5, Figures S33 and S34). We observed an increase in apparent rate constants of the thermal isomerization of **2-SP** upon the addition of CTAB, and a decrease in the apparent rate constant with the addition of SDS (Supporting Information-5.5, Table S8). We also monitored the change in zeta potential during these processes (Supporting Information-6.5, Figure S46). All cases follow the same trend where the zeta potential decreases upon irradiation and gradually recovers to the original value in the dark. The zeta potential of the **2**-CTAB co-assembly is less negative throughout the entire process, while in the presence of SDS the value is more negative. Positively charged CTAB would alleviate the repulsion between anionic **2-SP** and stabilize the self-assembly. Incorporating negatively charged SDS would need more zwitterionic **2-MCH** to be formed to overcome the coulombic repulsion, leading to a longer time for the required concentration of **2-MCH** to be reached. The shorter delay upon the addition of a cationic surfactant and the longer delay in the presence of an anionic surfactant are consistent with the balance of charge being important in the formation of these stable assemblies.

2.6. Reversibility of the System

To examine the reversibility of our system, samples of **2** were subjected to repeated switching cycles of 5 minutes of irradiation at 467 nm, followed by 85 minutes in the dark. The stability of the system was monitored by UV-vis spectroscopy (Figure 6). The time between the light being switched off and the increase in absorbance at 250 nm gradually gets longer after each cycle. The degradation of compound **2** could be a contributing factor, although initially unexpected as the parent merocyanine **1** is stable through multiple switching cycles.[21] Hydrolysis is usually expected to occur at higher pH[22a] (Supporting Information-12, Figure S60), but the observed absorption shoulder at 520 nm, consistent with the formation of **2-MC**, does suggest a possible hydrolysis route even at low pH.

When 0.1 eq. of CTAB is added, the rapid increase in absorbance at 250 nm still occurs over multiple cycles, suggesting a more consistent reformation of the assemblies. The decrease in absorbance at 250 nm after the self-assembly

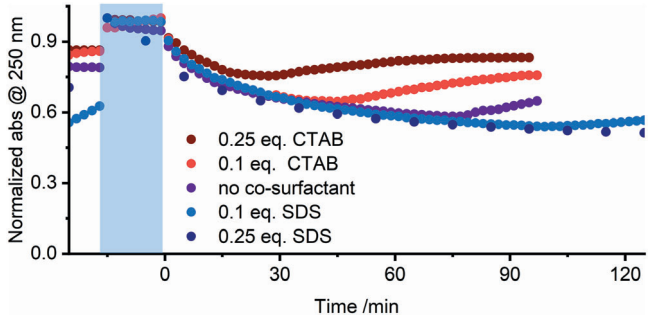

Figure 5. Recovery of absorbance at 250 nm, characteristic of **2-SP**, normalized to the highest absorbance of each trace (raw data presented in Supporting Information-5.5, Figure S33, S34) after irradiation with various amounts of co-surfactant added. Experimental conditions: [compound **2**] = 190 μM, 0.5% DMSO/water; pH = 4.8, [phosphate buffer] = 20 mM, T = 25 °C, irradiation time = 15 min, λ = 467 nm.

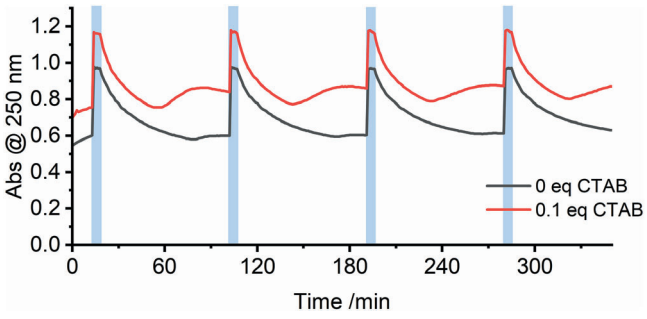

Figure 6. Change in characteristic absorbance of **1-SP** (250 nm) with (red) and without (black) 0.1 eq CTAB (0.19 μM) over multiple cycles. Irradiation time is indicated by the light blue rectangles. Experimental conditions: [compound **2**] = 190 μM, [phosphate buffer] = 20 mM, pH = 4.8, irradiation time = 5 min, λ = 467 nm, dark time = 85 min, T = 25 °C.

reformed indicates that more complex behavior occurs when the structures assemble, continuing to change the optical and thermal properties of the photoswitches over time.

3. Conclusion

We report a merocyanine-based amphiphile that self-assembles into light-responsive ellipsoids with complex equilibration behavior in the dark. The **2-SP** form ring-opens to form **2-MCH**, and together these assemble to form structures that stabilize the **2-SP** form. The isomerization rate and the photoswitching properties of the photoswitch are also significantly different when self-assembled compared to in dilute solution, which is probably true for most photoswitches. Under the conditions we studied, the amphiphiles abruptly self-assemble to form ellipsoids after a delay of ~70 minutes after the light was switched off. This delay was largely independent of the concentration but could be manipulated by incorporating simple co-surfactants of different charges. A deeper understanding of the underlying mechanism of the disassembly/assembly of these types of supramolecular structures, and how this impacts their responsive properties, will assist the design of functional materials. We anticipate that light-responsive assemblies of this size will enable spatiotemporally controlled cargo delivery with broad potential in targeted therapy, imaging, oscillating systems,[34] and beyond.

Supporting Information

Additional references cited within the Supporting Information.[35] The data supporting this article has been included as part of the ESI. Deposition Number 2452517 (for compound **2**) contains the supplementary crystallographic data for this paper. These data are provided free of charge by the joint Cambridge Crystallographic Data Centre and Fachinformationszentrum Karlsruhe Access Structures service. All data for this work is deposited on the ChemRxiv server, see DOI: 10.26434/chemrxiv-2025-qwl4n-v3.

Acknowledgments

The Australian Research Council is acknowledged for funding (DP220101847, DP250100041), The Mark Wainwright Analytical Centre's NMR, Electron Microscopy and Flow Cytometry facilities, Katelyn Clutterbuck for collecting X-ray crystal data, Dr Juanfang Ruan for collecting the CryoTEM images, and Dr Andrew J Clulow for assistance in SAXS data collection and analysis. This research was undertaken on the BioSAXS beamline (proposal 23911) and the MX1 beamlines (CAP19108) at the Australian Synchrotron, part of ANSTO, and made use of the Australian Cancer Research Foundation (ACRF) detector. The authors acknowledge the support of the Australian Centre for Neutron Scattering, ANSTO and the Australian Government through the National Collaborative Research Infrastructure Strategy (proposal 18538).

Open access publishing facilitated by University of New South Wales, as part of the Wiley - University of New South Wales agreement via the Council of Australian University Librarians.

Conflict of Interest

The authors declare no conflict of interest.

Data Availability Statement

The data that support the findings of this study are openly available in ChemRxiv at https://doi.org/10.26434/chemrxiv-2025-qwl4n-v2.

Keywords: amphiphile · photoswitch · self-assembly · spiropyran · supramolecular

[1] a) M. C. Branco, J. P. Schneider, *Acta Biomater.* **2009**, *5*, 817; b) N. Fomina, J. Sankaranarayanan, A. Almutairi, *Adv. Drug Deliv. Rev* **2012**, *64*, 1005.
[2] C. Li, A. Iscen, H. Sai, K. Sato, N. A. Sather, S. M. Chin, Z. Alvarez, L. C. Palmer, G. C. Schatz, S. I. Stupp, *Nat. Mater.* **2020**, *19*, 900.
[3] L. Su, J. Mosquera, M. F. J. Mabesoone, S. M. C. Schoenmakers, C. Muller, M. E. J. Vleugels, S. Dhiman, S. Wijker, A. R. A. Palmans, E. W. Meijer, *Science* **2022**, *377*, 213.
[4] a) Q. Duan, Y. Cao, Y. Li, X. Hu, T. Xiao, C. Lin, Y. Pan, L. Wang, *J. Am. Chem. Soc.* **2013**, *135*, 10542; b) Y. Cao, X. Y. Hu, Y. Li, X. Zou, S. Xiong, C. Lin, Y. Z. Shen, L. Wang, *J. Am. Chem. Soc.* **2014**, *136*, 10762.
[5] a) T. S. Davies, A. M. Ketner, S. R. Raghavan, *J. Am. Chem. Soc.* **2006**, *128*, 6669; b) X. Ji, M. Tian, Y. Wang, *Langmuir* **2016**, *32*, 972.
[6] a) Y. Zhang, W. Kong, C. Wang, P. An, Y. Fang, Y. Feng, Z. Qin, X. Liu, *Soft Matter* **2015**, *11*, 7469; b) J. Jiang, D. Zhang, J. Yin, Z. Cui, *Soft Matter* **2017**, *13*, 6458.
[7] S. Chen, R. Costil, F. K. Leung, B. L. Feringa, *Angew. Chem., Int. Ed.* **2021**, *60*, 11604.
[8] a) X. Liu, N. L. Abbott, *J. Colloid Interface Sci.* **2009**, *339*, 1; b) M. Kathan, S. Hecht, *Chem. Soc. Rev.* **2017**, *46*, 5536.
[9] a) T. Hayashita, T. Kurosawa, T. Miyata, K. Tanaka, M. Igawa, *Colloid. Polym. Sci.* **1994**, *272*, 1611; b) H. Sakai, A. Matsumura, S. Yokoyama, T. Saji, M. Abe, *J. Phys. Chem. B* **1999**, *103*, 10737; c) A. L. Le Ny, C. T. Lee, Jr., *J. Am. Chem. Soc.* **2006**, *128*, 6400; d) Y. C. Liu, A. L. Le Ny, J. Schmidt, Y. Talmon, B. F. Chmelka, C. T. Lee, Jr., *Langmuir* **2009**, *25*, 5713; e) C. Pernpeintner, J. A. Frank, P. Urban, C. R. Roeske, S. D. Pritzl, D. Trauner, T. Lohmuller, *Langmuir* **2017**, *33*, 4083; f) C. S. G. Butler, L. W. Giles, A. V. Sokolova, L. de Campo, R. F. Tabor, K. L. Tuck, *Langmuir* **2022**, *38*, 7522; g) C. Blayo, B. E. Jones, M. J. Bennison, R. C. Evans, *Org. Biomol. Chem.* **2024**, *23*, 138.
[10] a) G. Tyagi, J. L. Greenfield, B. E. Jones, W. N. Sharratt, K. Khan, D. Seddon, L. A. Malone, N. Cowieson, R. C. Evans, M. J. Fuchter, J. T. Cabral, *JACS Au* **2022**, *2*, 2670; b) I. Pani, M. Hardt, D. Glikman, B. Braunschweig, *Chem. Sci.* **2024**, *15*, 18865.
[11] J. C. Yau, K. L. Hung, Y. Ren, T. Kajitani, M. C. A. Stuart, F. K. Leung, *J. Colloid Interface Sci.* **2024**, *662*, 391.
[12] a) J. T. van Herpt, J. Areephong, M. C. Stuart, W. R. Browne, B. L. Feringa, *Chem.- Eur. J.* **2014**, *20*, 1737; b) Y. Kotani, H. Yasuda, K. Higashiguchi, K. Matsuda, *Chem.- Eur. J.* **2021**, *27*, 11158.
[13] a) Q. Chen, Y. Feng, D. Q. Zhang, G. X. Zhang, Q. H. Fan, S. N. Sun, D. B. Zhu, *Adv. Funct. Mater.* **2010**, *20*, 36; b) R. Tong, H. D. Hemmati, R. Langer, D. S. Kohane, *J. Am. Chem. Soc.* **2012**, *134*, 8848; c) R. Klajn, *Chem. Soc. Rev.* **2014**, *43*, 148; d) S. Son, E. Shin, B.-S. Kim, *Biomacromolecules* **2014**, *15*, 628; e) S. Kwangmettatam, T. Kudernac, *Chem. Commun.* **2018**, *54*, 5311; f) L. Kortekaas, W. R. Browne, *Chem. Soc. Rev.* **2019**, *48*, 3406; g)

Y. W. Zhang, M. Ng, E. Y. H. Hong, A. K. W. Chan, N. M. W. Wu, M. H. Y. Chan, L. X. Wu, V. W. W. Yam, *J. Mater. Chem. C* **2020**, *8*, 13676; h) M. Schnurbus, M. Kabat, E. Jarek, M. Krzan, P. Warszynski, B. Braunschweig, *Langmuir* **2020**, *36*, 6871; i) M. Reifarth, M. Bekir, A. M. Bapolisi, E. Titov, F. Nusshardt, J. Nowaczyk, D. Grigoriev, A. Sharma, P. Saalfrank, S. Santer, M. Hartlieb, A. Boker, *Angew. Chem., Int. Ed.* **2022**, *61*, e202114687; j) S. Qi, X. Lu, W. Mei, G. Gu, W. Li, A. Zhang, *Nanoscale* **2023**, *15*, 18053; k) A. Gao, F. X. Sun, Y. L. Duan, Y. X. Zhang, X. L. Liu, T. B. Liu, Y. H. Ji, Q. Y. Wu, X. Deng, Y. H. Zheng, C. Wei, D. S. Wang, *Adv. Funct. Mater.* **2024**, *34*, 2316457; l) J. Kim, H. Yun, Y. J. Lee, J. Lee, S.-H. Kim, K. H. Ku, B. J. Kim, *J. Am. Chem. Soc.* **2021**, *143*, 13333; m) D. A. Holden, H. Ringsdorf, V. Deblauwe, G. Smets, *J. Phys. Chem.* **1984**, *88*, 716; n) K. J. Tangso, W.-K. Fong, T. Darwish, N. Kirby, B. J. Boyd, T. L. Hanley, *J. Phys. Chem. B* **2013**, *117*, 10203.

[14] A. B. Grommet, L. M. Lee, R. Klajn, *Acc. Chem. Res.* **2020**, *53*, 2600.

[15] a) J. Wang, L. Avram, Y. Diskin-Posner, M. J. Białek, W. Stawski, M. Feller, R. Klajn, *J. Am. Chem. Soc.* **2022**, *144*, 21244; b) D. Samanta, D. Galaktionova, J. Gemen, L. J. W. Shimon, Y. Diskin-Posner, L. Avram, P. Král, R. Klajn, *Nat. Commun.* **2018**, *9*, 641.

[16] a) K. Dąbrowa, P. Niedbała, J. Jurczak, *Chem. Commun.* **2014**, *50*, 15748; b) S. J. Wezenberg, *Chem. Commun.* **2022**, *58*, 11045.

[17] R. G. DiNardi, A. O. Douglas, R. Tian, J. R. Price, M. Tajik, W. A. Donald, J. E. Beves, *Angew. Chem., Int. Ed.* **2022**, *61*, e202205701.

[18] a) J. Calbo, C. E. Weston, A. J. P. White, H. S. Rzepa, J. Contreras-García, M. J. Fuchter, *J. Am. Chem. Soc.* **2017**, *139*, 1261; b) B. Koeppe, F. Römpp, *Chem.– Eur. J.* **2018**, *24*, 14382; c) A. Dolai, S. M. Box, S. Bhunia, S. Bera, A. Das, S. Samanta, *J. Org. Chem.* **2023**, *88*, 8236.

[19] a) R. F. Tabor, M. J. Pottage, C. J. Garvey, B. L. Wilkinson, *Chem. Commun.* **2015**, *51*, 5509; b) R. Lund, G. Brun, E. Chevallier, T. Narayanan, C. Tribet, *Langmuir* **2016**, *32*, 2539; c) E. A. Kelly, J. E. Houston, R. C. Evans, *Soft Matter* **2019**, *15*, 1253; d) V. A. Bjornestad, X. Li, C. Tribet, R. Lund, M. Cascella, *J. Colloid Interface Sci.* **2023**, *646*, 883.

[20] a) J. Royes, V. A. Bjornestad, G. Brun, T. Narayanan, R. Lund, C. Tribet, *J. Colloid Interface Sci.* **2022**, *610*, 830; b) H. Iwase, M. Akamatsu, Y. Inamura, Y. Sakaguchi, K. Kobayashi, H. Sakai, *Langmuir* **2023**, *39*, 12357; c) J. H. Wei, J. Xing, X. F. Hou, X. M. Chen, Q. Li, *Adv. Mater.* **2024**, *36*, 2411291.

[21] L. Wimberger, J. Andréasson, J. E. Beves, *Chem. Commun.* **2022**, *58*, 5610.

[22] a) C. Berton, D. M. Busiello, S. Zamuner, E. Solari, R. Scopelliti, F. Fadaei-Tirani, K. Severin, C. Pezzato, *Chem. Sci.* **2020**, *11*, 8457; b) L. Wimberger, S. K. K. Prasad, M. D. Peeks, J. Andreasson, T. W. Schmidt, J. E. Beves, *J. Am. Chem. Soc.* **2021**, *143*, 20758.

[23] e.g. 20 μM, $t_{\frac{1}{2}} = 16$ min (pH 3); 8 min (pH 4); 4.7 min (pH 6), see SI-4.2.

[24] A small proportion of DMSO is required to dissolve compound **2** (SI-3.1).

[25] F. Jonsson, T. Beke-Somfai, J. Andréasson, B. Nordén, *Langmuir* **2013**, *29*, 2099.

[26] M. Bekir, M. Schenderlein, J. Ruickoldt, P. Wendler, J. Kohlbrecher, I. Hoffmann, M. Reifarth, *Chem. Commun.* **2025**, *61*, 5585.

[27] X. M. Chen, X. F. Hou, H. K. Bisoyi, W. J. Feng, Q. Cao, S. Huang, H. Yang, D. Chen, Q. Li, *Nat. Commun.* **2021**, *12*, 4993.

[28] M. Hammarson, J. R. Nilsson, S. Li, T. Beke-Somfai, J. Andréasson, *J. Phys. Chem. B* **2013**, *117*, 13561.

[29] a) I. F. Uchegbu, J. A. Bouwstra, A. T. Florence, *J. Phys. Chem.* **1992**, *96*, 10548; b) A. G. Daful, J. B. Avalos, A. D. Mackie, *Langmuir* **2012**, *28*, 3730; c) S. E. Anachkov, P. A. Kralchevsky, K. D. Danov, G. S. Georgieva, K. P. Ananthapadmanabhan, *J. Colloid Interface Sci.* **2014**, *416*, 258; d) E. J. Dufourc, *Biochim. Biophys. Acta – Biomembr.* **2021**, *1863*, 183478; e) G. Rodríguez, G. Soria, E. Coll, L. Rubio, L. Barbosa-Barros, C. López-Iglesias, A. M. Planas, J. Estelrich, A. de la Maza, O. López, *Biophys. J.* **2010**, *99*, 480; f) L. Rubio, C. Alonso, G. Rodríguez, L. Barbosa-Barros, L. Coderch, A. De la Maza, J. L. Parra, O. López, *Int. J. Pharm.* **2010**, *386*, 108.

[30] L. Kortekaas, J. D. Steen, D. R. Duijnstee, D. Jacquemin, W. R. Browne, *J. Phys. Chem. A* **2020**, *124*, 6458.

[31] We observe that **2-MCH** is also weakly emissive, but its emission energy appears to be independent of its aggregation state (SI-10).

[32] T. Kunitake, *Angew. Chem., Int. Ed.* **1992**, *31*, 709.

[33] a) K. Shirahama, M. Hayashi, R. Matuura, *Bull. Chem. Soc. Jpn.* **1969**, *42*, 1206; b) A. Cifuentes, J. L. Bernal, J. C. DiezMasa, *Anal. Chem.* **1997**, *69*, 4271; c) A. Rahman, C. W. Brown, *J. Appl. Polym. Sci.* **2003**, *28*, 1331.

[34] M. G. Howlett, A. H. J. Engwerda, R. J. H. Scanes, S. P. Fletcher, *Nat. Chem* **2022**, *14*, 805.

[35] a) N. Mallo, E. D. Foley, H. Iranmanesh, A. D. W. Kennedy, E. T. Luis, J. Ho, J. B. Harper, J. E. Beves, *Chem. Sci.* **2018**, *9*, 8242; b) E. I. Balmond, B. K. Tautges, A. L. Faulkner, V. W. Or, B. M. Hodur, J. T. Shaw, A. Y. Louie, *J. Org. Chem.* **2016**, *81*, 8744; c) R. Colaco, S. Shree, L. Siebert, C. Appiah, M. Dowds, S. Schultzke, R. Adelung, A. Staubitz, *ACS Appl. Polym. Mater.* **2020**, *2*, 2055; d) N. A. Voloshin, A. V. Metelitsa, J. C. Micheau, E. N. Voloshina, S. O. Besugliy, A. V. Vdovenko, N. E. Shelepin, V. I. Minkin, *Russ. Chem. Bull.* **2003**, *52*, 1172; e) T. M. McPhillips, S. E. McPhillips, H. J. Chiu, A. E. Cohen, A. M. Deacon, P. J. Ellis, E. Garman, A. Gonzalez, N. K. Sauter, R. P. Phizackerley, S. M. Soltis, P. Kuhn, *J. Synchrotron Rad.* **2002**, *9*, 401; f) W. Kabsch, *Acta Crystallogr. D. Biol. Crystallogr.* **2010**, *66*, 125; g) G. M. Sheldrick, *Acta Crystallogr. A: Found. Crystallogr.* **2008**, *64*, 112; h) G. M. Sheldrick, *Acta crystallogr. C: Struct. Chem.* **2015**, *71*, 3; i) O. V. Dolomanov, L. J. Bourhis, R. J. Gildea, J. A. K. Howard, H. Puschmann, *J. Appl. Crystallogr.* **2009**, *42*, 339; j) A. L. Spek, *Acta Crystallogr Commun* **2020**, *76*, 1; k) A. Sokolova, J. Christoforidis, A. Eltobaji, J. Barnes, F. Darmann, A. E. Whitten, L. d. Campo, *Neutron News* **2016**, *27*, 9; l) A. Sokolova, A. E. Whitten, L. de Campo, J. Christoforidis, A. Eltobaji, J. Barnes, F. Darmann, A. Berry, *J. Appl. Crystallogr.* **2019**, *52*, 1; m) O. Arnold, J. C. Bilheux, J. M. Borreguero, A. Buts, S. I. Campbell, L. Chapon, M. Doucet, N. Draper, R. F. Leal, M. A. Gigg, V. E. Lynch, A. Markvardsen, D. J. Mikkelson, R. L. Mikkelson, R. Miller, K. Palmen, P. Parker, G. Passos, T. G. Perring, P. F. Peterson, S. Ren, M. A. Reuter, A. T. Savici, J. W. Taylor, R. J. Taylor, R. Tolchenov, W. Zhou, J. Zikovsky, *Nucl. Instrum. Methods Phys. Res. A: Accel. Spectrom. Detect. Assoc. Equip.* **2014**, *764*, 156; n) A. Guinier, G. Fournet, C. B. Walker, K. L. Yudowitch, *Small-angle Scattering of X-rays*, Wiley New York, **1955**; o) A. Isihara, *J. Chem. Phys.* **1950**, *18*, 1446; p) L. Feigin, D. I. Svergun, *Structure analysis by small-angle X-ray and neutron scattering, Vol. 1*, Springer, New York, **1987**; q) A. L. Buckinx, L. J. Weerarathna, A. Sokolova, T. Junkers, *Polym. Chem.* **2024**, *15*, 4615; r) Y.-R. E. Tan, S. Porsa, D. Zhu, C. Kamma-Lorger, A. J. Clulow, S. Casalbuoni, A. Grau, N. Glamann, A. Hobl, M. Krichler, *J. Synchrotron Rad.* **2025**, *32*, 908; s) D. Kim, Z. Zhang, K. Xu, *J. Am. Chem. Soc.* **2017**, *139*, 9447.

Manuscript received: July 29, 2025
Revised manuscript received: August 5, 2025
Version of record online: August 19, 2025